Introduction to Percolation Theory (Part A)

Armin Bunde and Jan W. Kantelhardt

1.1 Introduction

Percolation is a standard model for disordered systems. Its applications range from transport in amorphous and porous media and composites to the properties of branched polymers, gels and complex ionic conductors. Because of universality the results do not depend on the specific model, and general scaling laws can be deduced. In the first part of this chapter we give a short introduction to percolation theory and describe one application to composites. We start with the structural properties of percolation clusters and their substructures at criticality. Then we turn to the dynamical properties of percolation clusters and discuss the way the laws of diffusion and conduction are modified on percolation structures. Finally, we review a particular application of the percolation concept, ionic diffusion in dispersed ionic conductors.

In the second part of the chapter, electrical conduction in laser-irradiated polymers will be discussed by R. Sauerbrey and E. Welsch.

1.2 The (site-)percolation model

Percolation represents the basic model for a structurally disordered system (for recent reviews see [1, 2], for applications see [3]). Let us consider a square lattice, where each site is occupied randomly with probability p or is empty with probability $1 - p$ (see fig. 1). Occupied and empty sites may stand for very different physical properties. For illustration, let us assume that the occupied sites are electrical conductors, the empty sites represent insulators, and that electrical current can only flow between nearest-neighbour conductor sites.

At low concentration p, the conductor sites are either isolated or form small clusters of nearest-neighbour sites. Two conductor sites belong to the same cluster if they are connected by a path of nearest-neighbour conductor sites, and a current can flow between them. At low p values, the mixture is an insulator, since no conducting path connecting opposite edges of our lattice exists. At large p values on the other hand many conducting paths between opposite edges exist, where electrical current can flow, and the mixture is a conductor. At some concentration in between, therefore, a threshold concentration p_c must exist where for the first time electrical current can *percolate* from one edge to the other. Below p_c we have an insulator, above p_c we have a conductor. The threshold

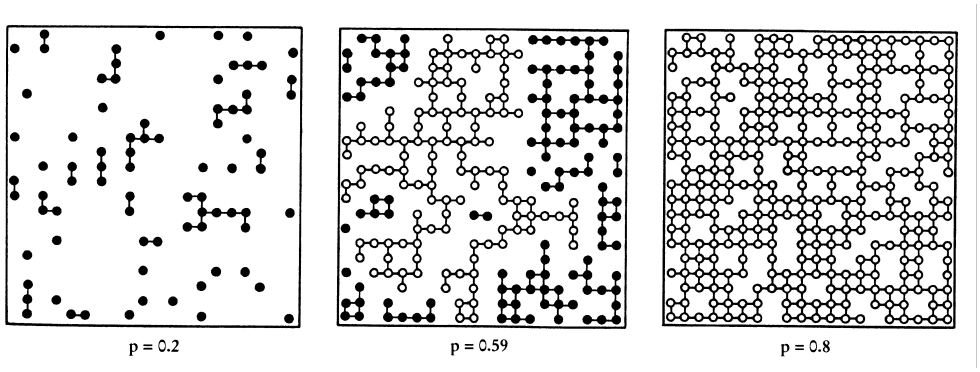

Figure 1 Site percolation on the square lattice: The small circles represent the occupied sites for three different concentrations: $p = 0.2$, 0.59, and 0.80. Nearest-neighbour cluster sites are connected by lines representing the bonds. Filled circles are used for finite clusters, while open circles mark the large *infinite* cluster.

concentration is called the *percolation threshold,* or, since it separates two different phases, the *critical concentration.*

If the occupied sites are superconductors and the empty sites are conductors, p_c separates a normal-conducting phase below p_c from a superconducting phase above p_c. Another example is a mixture of ferromagnets and paramagnets, where the system changes at p_c from paramagnetic to ferromagnetic.

In contrast to the more common thermal phase transitions, where the transition between two phases occurs at a critical temperature, the *percolation transition* described here is a *geometrical phase transition,* which is characterized by the geometric features of large clusters in the neighbourhood of p_c. At low values of p only small clusters of occupied sites exist. When the concentration p is increased the average size of the clusters increases. At the critical concentration p_c a large cluster appears which connects opposite edges of the lattice. We call this cluster the *infinite* cluster, since its size diverges in the thermodynamic limit. When p is increased further the density of the infinite cluster increases, since more and more sites become part of the infinite cluster, and the average size of the *finite* clusters, which do not belong to the infinite cluster, decreases. At $p = 1$, trivially, all sites belong to the infinite cluster.

The critical concentration depends on the details of the lattice and increases, for fixed dimension d of the lattice, with decreasing coordination number z of the lattice: For the triangular lattice, $z = 6$ and $p_c = 1/2$, for the square lattice, $z = 4$ and $p_c \cong 0.592746$, and for the honeycomb lattice, $z = 3$ and $p_c \cong 0.6962$. For fixed z, p_c decreases if the dimension d is enhanced. In both the triangular lattice and the simple cubic lattice we have $z = 6$, but p_c for the simple cubic lattice is considerably smaller, $p_c \cong 0.3116$.

The percolation transition is characterized by the geometrical properties of the clusters near p_c [1,2]. The probability P_∞ that a site belongs to the infinite cluster is zero below p_c and increases above p_c as

$$P_\infty \sim (p - p_c)^\beta. \tag{1}$$

This behaviour is illustrated in fig. 2. The linear size of the *finite* clusters, below and above p_c, is characterized by the *correlation length* ξ. The correlation length is defined

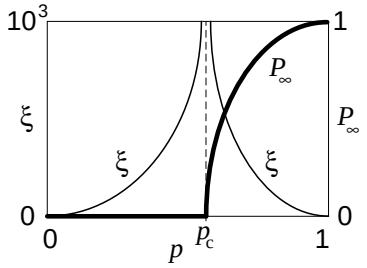

Figure 2 Schematic diagram of the probability P_∞ (eq. (1), bold line) and the correlation length ξ (eq. (2), thin line) versus the concentration p of occupied sites.

as the mean distance between two sites on the same finite cluster and represents the characteristic length scale in percolation. When p approaches p_c, ξ increases as

$$\xi \sim \mid p - p_c \mid^{-\nu}, \tag{2}$$

with the same exponent ν below and above the threshold (see also fig. 2). While p_c depends explicitly on the type of the lattice, the *critical exponents* β and ν are universal and depend only on the dimension d of the lattice, but not on the type of the lattice. The values of the critical exponents are given in table 1 for two and three dimensions.

1.3 The fractal structure of percolation clusters near p_c

Near p_c on length scales smaller than ξ both the infinite cluster and the finite clusters are self-similar, i.e., if we cut a small part out of a large cluster, magnify it to the original cluster size and compare it with the original, we cannot tell the difference: Both look the same. This feature is illustrated in fig. 3, where a large cluster at p_c is shown in four different magnifications. We leave it to the reader to find out what is the original and what are the magnifications.

Table 1 Critical exponents and fractal dimensions for percolation in two and three dimensions. The numerical values are taken from [1].

Quantity		Exponent	$d = 2$	$d = 3$
Order parameter	$P_\infty(p) \sim (p - p_c)^\beta$	β	$5/36$	0.417 ± 0.003
Correlation length	$\xi(p) \sim \mid p - p_c \mid^{-\nu}$	ν	$4/3$	0.875 ± 0.008
Cluster mass	$M(r) \sim r^{d_f}$	d_f	$91/48$	2.524 ± 0.008
Backbone mass	$M_B(r) \sim r^{d_B}$	d_B	1.62 ± 0.02	1.855 ± 0.015
Chemical Path	$\ell(r) \sim r^{d_{\min}}$	$d_{\min}$	1.13 ± 0.004	1.374 ± 0.004
Random Walk	$\langle r^2(t) \rangle \sim t^{2/d_w}$	d_w	2.871 ± 0.001	3.80 ± 0.02
Conductivity	$\sigma_{\rm dc}(p) \sim (p_c - p)^\mu$	μ	1.30 ± 0.002	1.99 ± 0.01
Superconductivity	$\sigma_{\rm S}(p) \sim (p - p_c)^{-s}$	s	1.30 ± 0.002	0.74 ± 0.03

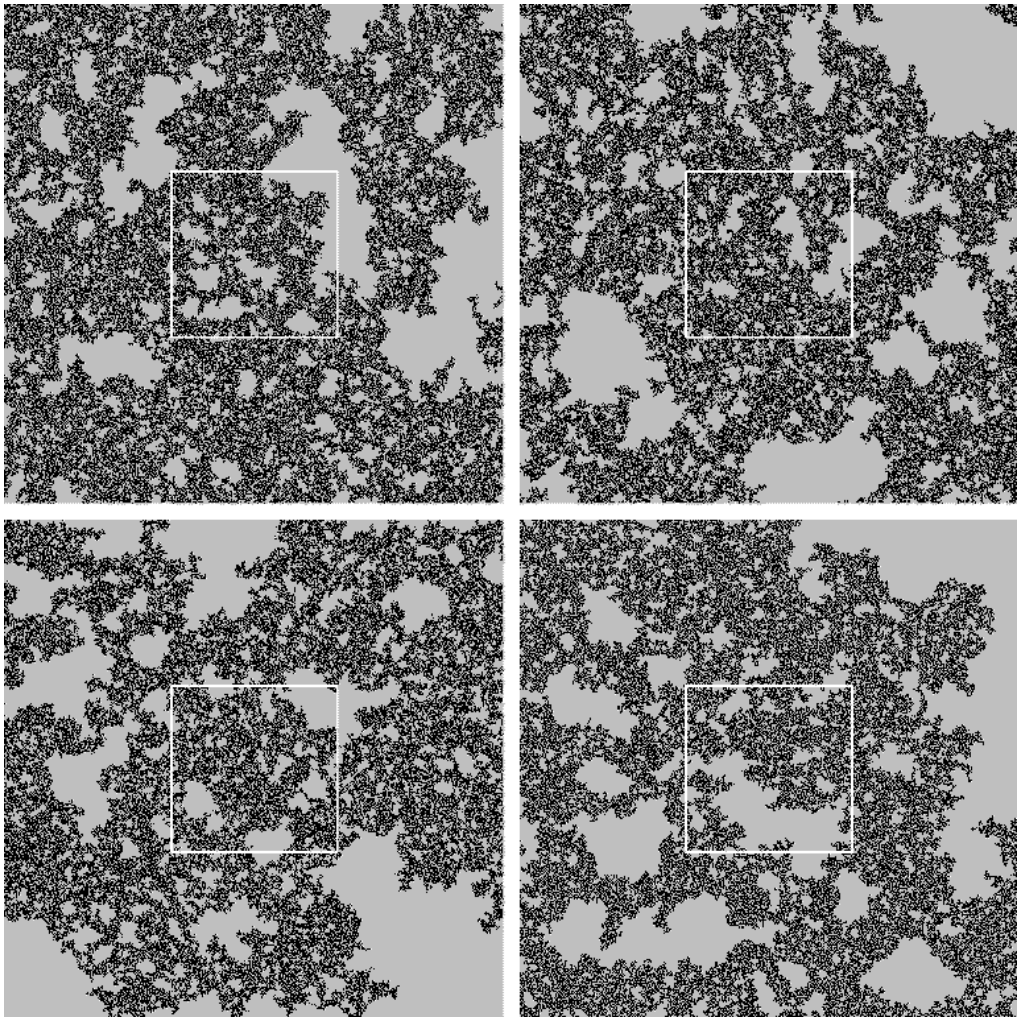

Figure 3 Self-similarity of a large percolation cluster on the square lattice at the critical concentration. Three of the clusters are magnifications of the center parts marked by white squares.

We have learnt in chapter 13 that – as a consequence of the (non-trivial) self-similarity – the cluster is characterized by a "fractal" dimension, which is smaller than the dimension d of the embedding lattice. The mean mass of the cluster within a circle of radius r increases with r as

$$M(r) \sim r^{d_f}, \qquad r \ll \xi, \tag{3}$$

with the "fractal dimension" d_f. The numerical values of d_f can be found in table 1. Above p_c on length scales *larger* than ξ the infinite cluster can be regarded as an homogeneous system which is composed of many cells of size ξ. Mathematically, this can be summarized as

$$M(r) \sim \begin{cases} r^{d_f}, & \text{if } r \ll \xi, \\ r^d, & \text{if } r \gg \xi. \end{cases} \tag{4}$$

The fractal dimension d_f can be related to β and ν in the following way: Above p_c, the mass M_∞ of the infinite cluster in a large lattice of size L^d is proportional to $L^d P_\infty$. On the other hand, this mass is also proportional to the number of unit cells of size ξ, $(L/\xi)^d$, multiplied by the mass of each cell which is proportional to ξ^{d_f}. This yields (with eqs. (1) and (2))

$$M_\infty \sim L^d P_\infty \sim L^d (p - p_c)^\beta \sim (L/\xi)^d \xi^{d_f} \sim L^d (p - p_c)^{\nu d - \nu d_f}, \tag{5}$$

and hence, comparing the exponents of $(p - p_c)$,

$$d_f = d - \frac{\beta}{\nu}. \tag{6}$$

Since β and ν are universal exponents, d_f is also universal.

A fractal percolation cluster is composed of several fractal substructures, which are described by other exponents [1, 2]. Imagine applying a voltage between two sites at opposite edges of a metallic percolation cluster: The *backbone* of the cluster consists of those sites (or bonds) which carry the electric current. The *topological distance* between both points (also called chemical distance) is the length of the shortest path on the cluster connecting them. The *dangling ends* are those parts of the cluster which carry no current and are connected to the backbone by a single site only. The *red bonds* (or singly connected bonds), finally, are those bonds that carry the total current; when they are cut the current flow stops.

The fractal dimension d_B of the backbone is smaller than the fractal dimension d_f of the cluster, reflecting the fact that most of the mass of the cluster is concentrated in the dangling ends. On the average, the topological length ℓ of the path between two points on the cluster increases with the Euclidian distance r between them as $\ell \sim r^{d_{\min}}$. The values of the fractal dimensions d_B and $d_{\min}$ are given in table 1 for two and three dimensions. The fractal dimensions of the red bonds $d_{\rm red}$ are known from exact analytical arguments. The mean number of red bonds varies with p as $n_{\rm red} \sim (p - p_c)^{-1} \sim \xi^{1/\nu} \sim r^{1/\nu}$, and the fractal dimension of the red bonds is therefore $d_{\rm red} = 1/\nu$ [1].

A further important substructure of the cluster is the *external perimeter* (which is also called the *hull*). The hull consists of those sites of the cluster which are adjacent to empty sites and are connected with infinity via empty sites. It is an important model for random fractal interfaces. In two dimensions, the hull has the fractal dimension $d_h = 7/4$, while its mass seems to be proportional to the mass of the cluster in $d = 3$, i.e. $d_h = d_f$. In contrast to the hull, the *total perimeter* also includes the holes in the cluster.

1.4 Further percolation systems

So far we have considered *site percolation,* where the sites of a lattice have been occupied randomly. When the sites are all occupied, but the bonds between the sites are randomly occupied with probability q, we speak of *bond percolation* (see fig. 4a). Two occupied bonds belong to the same cluster if they are connected by a path of occupied bonds, and the critical concentration q_c of bonds ($q_c = 1/2$ in the square lattice and $q_c \simeq 0.2488$ in the simple cubic lattice) separates a phase of finite clusters of bonds from a phase with an infinite cluster [1, 2].

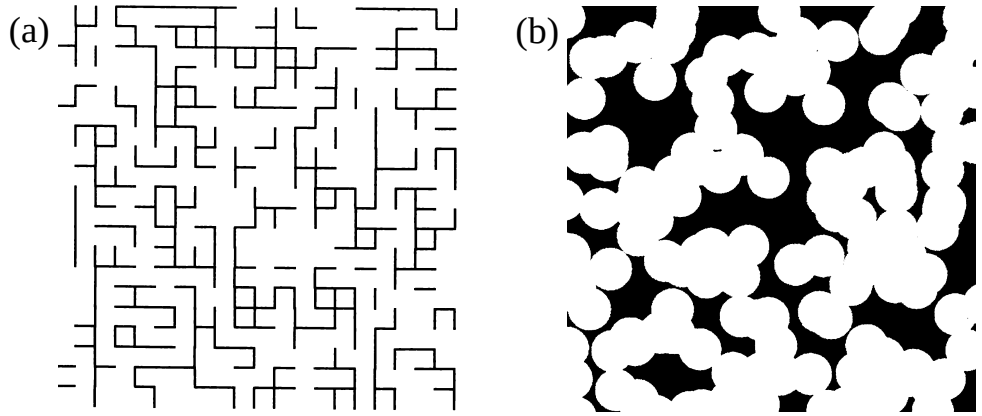

Figure 4 Further percolation systems: (a) Bond percolation cluster on a square lattice and (b) continuum percolation of circular discs with fixed radius at the percolation threshold.

If sites are occupied with probability p *and* bonds are occupied with probability q, we speak of *site–bond percolation.* Two occupied sites belong to the same cluster if they are connected by a path of nearest-neighbour occupied sites with occupied bonds in between. For $q = 1$, site–bond percolation reduces to site percolation, for $p = 1$ it reduces to bond percolation. In general, both parameters characterize the state of the system. Accordingly, a *critical line* in (p,q) space separates both phases, which for $p = 1$ and $q = 1$ takes the values of the critical bond and site concentrations, respectively.

Perhaps the most common example of bond percolation in physics is a *random resistor network,* where the metallic wires in a regular network are cut randomly with probability $1 - q$. Here q_c separates a conductive phase at large q from an insulating phase at low q. A possible application of bond percolation in chemistry is the polymerization process, where small branching molecules can form large molecules by activating more and more bonds between them. If the activation probability q is above the critical concentration, a network of chemical bonds spanning the whole system can be formed, while below q_c only macromolecules of finite size can be generated. This process is called a *sol-gel* transition. An example of this *gelation* process is the boiling of an egg, which at room temperature is liquid and upon heating becomes a more solid-like *gel.* Site–bond percolations can be relevant for gelation in dilute media.

The most natural example of percolation is *continuum percolation,* where the positions of the two components of a random mixture are not restricted to the discrete sites of a regular lattice. As a simple example, consider a sheet of conductive material, with circular holes punched randomly in it (see fig. 4b). The relevant quantity now is the fraction p of remaining conductive material. Compared with site and bond percolation, the critical concentration is further decreased: $p_c \cong 0.312$ for $d = 2$, when all circles have the same radius. This picture can easily be generalized to three dimensions, where spherical voids are generated randomly in a cube, and $p_c \cong 0.034$. Due to its similarity to Swiss cheese, this model of continuous percolation is called the Swiss cheese model. Similar models, where also the size of the spheres can vary, are used to describe sandstone and other porous materials.

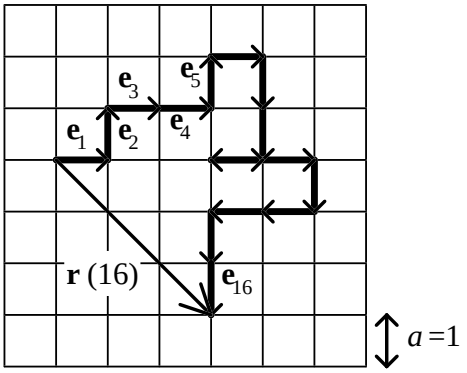

Figure 5 Random walk on a square lattice. The lattice constant $a = 1$ is equal to the jump length of the random walker. Sixteen steps of the walk are shown.

It is important that close to the percolation threshold all these different percolation systems are characterized by the same critical exponents β, ν, and d_f given in table 1. The exponents are universal and depend neither on the structural details of the lattice (e.g., square or triangular) nor on the type of percolation (site, bond, or continuum), but only on the dimension d of the lattice.

1.5 Diffusion on regular lattices

After we have discussed the structural properties of percolation systems close to the percolation threshold, we will now focus on the *dynamical* properties of percolation systems, where to each site or bond a physical property such as conductivity is assigned. We show that due to the fractal nature of the percolation clusters near p_c, the physical laws of dynamics are changed essentially and become *anomalous*.

At first, we consider regular lattices. The diffusion process is commonly modeled by a simple random walk (see e.g., chapters 12 and 13), which advances one step of length a in one time unit. Each step brings the random walker to a randomly chosen nearest-neighbour site on a given d-dimensional lattice. Assume that the walker starts at time $t = 0$ at the origin of the lattice. After t time steps, the actual position is described by the vector (see fig. 5)

$$\mathbf{r}(t) = a \sum_{\tau=1}^{t} \mathbf{e}_\tau, \tag{7}$$

where $\mathbf{e}_\tau$ denotes the unit vector pointing in the direction of the jump at the τth time step.

The mean distance the random walker has travelled after t time steps is described by the root mean square displacement $R(t) \equiv \langle r^2(t) \rangle^{1/2}$, where the average $\langle \cdots \rangle$ is over all random-walk configurations on the lattice. From eq. (7) we obtain

$$\langle r^2(t) \rangle = a^2 \sum_{\tau,\tau'=1}^{t} \langle \mathbf{e}_\tau \cdot \mathbf{e}_{\tau'} \rangle = a^2 t + \sum_{\tau \neq \tau'} \langle \mathbf{e}_\tau \cdot \mathbf{e}_{\tau'} \rangle. \tag{8}$$

Since jumps at different steps τ and τ' are uncorrelated, we have $\langle \mathbf{e}_\tau \cdot \mathbf{e}_{\tau'} \rangle = \delta_{\tau\tau'}$, and we obtain the Einstein relation

$$\langle r^2(t) \rangle = a^2 t, \tag{9}$$

which is equivalent to Fick's first law (see section 6.2). Note that eq. (9) is independent of the dimension d of the lattice.

In the general case, when the lengths of the steps of the random walker may vary, eq. (9) is modified into

$$\langle r^2(t) \rangle = 2dDt, \tag{10}$$

where D is the *diffusion coefficient.* The diffusion coefficient is (approximately) related to the dc conductivity $\sigma_{\rm dc}$ by the Nernst-Einstein equation,

$$\sigma_{\rm dc} = n(e^2/k_B T)D, \tag{11}$$

where n is the density and e the charge of the diffusing particles.

A more complete description of the diffusion process is possible with the probability density $P(r,t)$, where $P(r,t)dr$ is the probability of finding the walker after t time steps at a site within distance r from its starting point. The mean square displacement can be obtained from $P(r,t)$ via $\langle r^2(t) \rangle = \int d\mathbf{r}\, r^2 P(r,t)$. For $t \gg r$, $P(r,t)$ is described by a Gaussian: $P(r,t) \cong \frac{1}{\sqrt{2\pi t}} e^{-r^2/2t}$. This 'normal' probability density characterizes the diffusion on regular lattices. Next we consider disordered structures.

1.6 Diffusion on percolation clusters

We start with the infinite percolation cluster at the critical concentration p_c. The cluster has loops and dangling ends, and both substructures slow down the motion of a random walker. Due to self-similarity, loops and dangling ends occur on all length scales, and therefore the motion of the random walker is slowed down on *all* length scales. The time t the walker needs to travel a distance R is no longer, as in regular systems, proportional to R^2, but scales as $t \sim R^{d_w}$, where $d_w > 2$ is the *fractal dimension of the random walk* [1,2]. For the mean-square displacement this yields immediately

$$\langle r^2(t) \rangle \sim t^{2/d_w}. \tag{12}$$

The fractal dimension d_w is approximately equal to $3d_f/2$ [4]; the results of numerical simulations can be found in table 1. For continuum percolation (Swiss cheese model) in $d = 3$, d_w is enhanced: $d_w \cong 4.2$ [5]. Diffusion processes described by eq. (12) are generally referred to as *anomalous diffusion* (cf. chapter 6).

The probability density $\langle P(r,t) \rangle_N$, averaged over N percolation clusters, is not so easy to calculate. Analytical expressions for $\langle P(r,t) \rangle_N$ that fully describe the data obtained from numerical simulations can be derived. The derivation is beyond the scope of this book and we refer the interested reader to [1,6].

Comparatively simple, however, is the scaling behaviour of $\langle P(0,t) \rangle$, which denotes the probability of being, after t time steps, at the site where the random walker started. Since for very large times each site has the same probability of being visited, the probability of being at the origin is proportional to the inverse of the number of distinct sites $S(t)$ the random walker visited. Since $S(t)$ increases with $R(t) \equiv \langle r^2(t) \rangle^{1/2}$ as $S(t) \sim R(t)^{d_f}$, we have

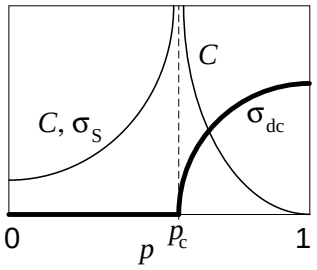

Figure 6 Schematic diagram of the (usual) dc conductivity $\sigma_{\rm dc}$ (eq. (15), bold line) and the conductivity σ_S for a conductor-superconductor percolation network (eq. (20), thin line for $p < p_c$) versus the concentration p of occupied sites. The cluster capacitance C is proportional to σ_S for $p < p_c$ and diverges with the same exponent for $p > p_c$ (see eq. (25)).

$$\langle P(0,t)\rangle \sim R(t)^{-d_f} \sim t^{-d_f/d_w} \tag{13}$$

(see also section 13.3).

Above p_c, fractal structures occur only within the correlation length $\xi(p)$ from eq. (2). Thus the anomalous diffusion law, eq. (12), occurs only below the corresponding crossover time $t_\xi \sim R(t_\xi)^{d_w} \sim \xi^{d_w}$, which decreases proportional to $(p-p_c)^{-\nu d_w}$, if p is further increased. Above t_ξ, on large time scales, the random walker explores large length scales where the cluster is homogeneous, and $\langle r^2(t)\rangle$ follows Fick's law (eqs. (9) or (10)) increasing linearly with time t. Thus,

$$\langle r^2(t)\rangle \sim \begin{cases} t^{2/d_w}, & \text{if } t \ll t_\xi, \\ t, & \text{if } t \gg t_\xi. \end{cases} \tag{14}$$

1.7 Conductivity of percolation clusters

The diffusion coefficient is related to the dc conductivity $\sigma_{\rm dc}$ by the Nernst-Einstein equation, eq. (11). Below p_c, there is no current between opposite edges of the system, and $\sigma_{\rm dc} = 0$. Above p_c, $\sigma_{\rm dc}$ increases by a power law (see fig. 6 for illustration),

$$\sigma_{\rm dc} \sim (p-p_c)^\mu, \tag{15}$$

where the critical exponent μ is (semi)-universal. For percolation on a lattice, μ depends only on d; the numerical results are contained in table 1. For continuum percolation (Swiss cheese model) in $d = 3$, however, μ is enhanced: $\mu \cong 2.38$.

Combining eqs. (11) and (15), we can obtain the behaviour of the diffusion coefficient D as a function of $p - p_c$. Since only the particles on the infinite cluster contribute to the dc conductivity, we have (from eq. (1)) $n \sim P_\infty \sim (p-p_c)^\beta$ in eq. (11). This yields

$$D \sim (p-p_c)^{\mu-\beta}. \tag{16}$$

Next we use scaling arguments to relate the exponent μ to d_w. Equations (16) and (10) imply that above t_ξ, the mean-square displacement $\langle r^2(t)\rangle$ behaves as

$$\langle r^2(t)\rangle \sim (p-p_c)^{\mu-\beta} t, \quad t > t_\xi. \tag{17}$$

On the other hand we know that for times below t_ξ on distances $r < t_\xi^{1/d_w}$,

$$\langle r^2(t)\rangle \sim t^{2/d_w}, \quad t < t_\xi. \tag{18}$$

By definition, for $t = t_\xi$, we have $\langle r^2(t)\rangle \sim \xi^2$. Substituting this into eqs. (17) and (18) and equating both relations we obtain immediately $(p-p_c)^{\mu-\beta} t_\xi \sim t_\xi^{2/d_w}$. Using $t_\xi \sim \xi^{d_w} \sim (p-p_c)^{-\nu d_w}$ (from eq. (2)) we get the relation between μ and d_w,

$$d_w = 2 + (\mu - \beta)/\nu. \tag{19}$$

1.8 Further electrical properties

In the last subsection we have already seen that the dc conductivity in the conductor-insulator system is zero below p_c and increases with a power law above p_c. If we consider, instead, the corresponding superconductor-conductor system, the conductivity is infinite above p_c and diverges with a power law when approaching p_c from below (see fig. 6),

$$\sigma_{\rm S} \sim (p_c - p)^{-s}. \tag{20}$$

The numerical results for s can be found in table 1.

Next, for generalizing this result and for obtaining further electric properties, let us assume that each bond in the network represents (with probability p) a circuit consisting of a resistor with resistivity $1/\sigma_A^0$ and a capacitor with capacitance C_A, or (with probability $1-p$) a circuit consisting of a resistor with resistivity $1/\sigma_B^0$ and a capacitor with capacitance C_B. The (complex) conductivity of each bond is therefore either $\sigma_A = \sigma_A^0 - i\omega C_A$ or $\sigma_B = \sigma_B^0 - i\omega C_B$. This model is called equivalent circuit model. At the percolation threshold the total conductivity follows a power-law [1, 7, 8],

$$\sigma(\omega) = \sigma_A (\sigma_A/\sigma_B)^{-u}, \tag{21}$$

where the exponent

$$u = \mu/(\mu + s) \tag{22}$$

is related to the exponents μ and s from above, $u = 0.5$ in $d = 2$ and $u \cong 0.71$ in $d = 3$ (see table 1).

For extending this result to the critical regime below and above p_c, we multiply eq. (21) by a complex scaling function $S(z)$ that depends on $z = |p - p_c|(\sigma_A/\sigma_B)^\Phi$ and can be different above and below p_c [9, 10],

$$\sigma(\omega) = \sigma_A (\sigma_A/\sigma_B)^{-u} \cdot S[|p - p_c|(\sigma_A/\sigma_B)^\Phi]. \tag{23}$$

The exponent Φ as well as the asymptotic behaviour of the scaling function is determined by the asymptotic behaviour of $\sigma(\omega)$ in the limit $\omega \to 0$ and $(\sigma_A/\sigma_B) \to \infty$.

In the following, let us concentrate on the conductor-capacitor limit, where $\sigma_A = \sigma_A^0$ and $\sigma_B = -i\omega C_B$. Then the complex scaling variable z is proportional to $|p - p_c|[\sigma_A^0/(-i\omega C_B)]^\Phi \sim (\tau\omega)^{-\Phi}$, and $\tau = |p-p_c|^{-1/\Phi} C_B/\sigma_A^0$ defines the characteristic time scale in this short-circuit model. Splitting the complex function $(-i)^u S(z)$ into its real part S_1 and imaginary part S_2, we obtain for the complex conductivity

$$\sigma(\omega) = \sigma_A^0 (C_B/\sigma_A^0)^u \cdot \omega^u \cdot [S_1(\tau\omega)] + iS_2(\tau\omega)], \tag{24}$$

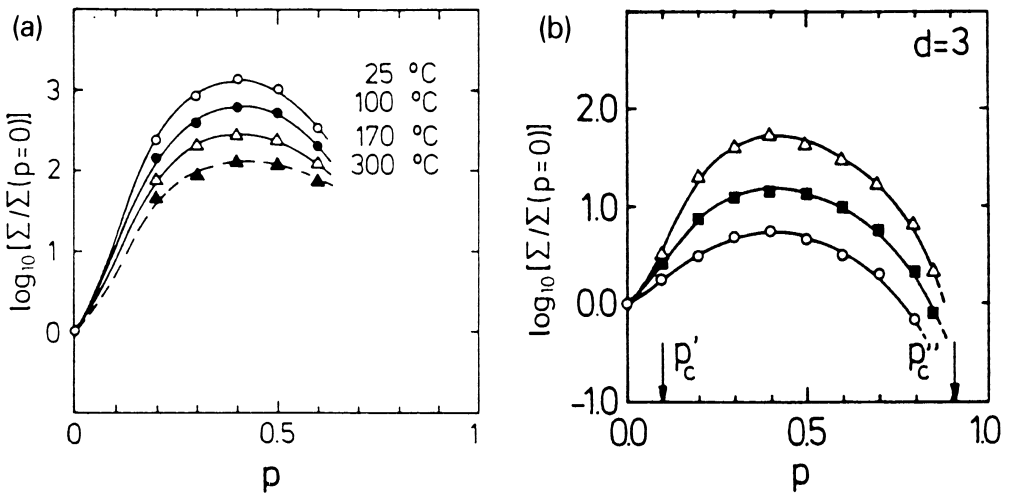

Figure 7 (a) Specific conductivity of the Li-Al_2O_3 system as a function of the mole fraction p of Al_2O_3 at different temperatures (after [11]). (b) Total conductivity resulting from Monte-Carlo-Simulations of the two-phase percolation model, as a function of p, for $\sigma_A^0/\sigma_B^0 = 10$ (circle), 30 (full square), and 100 (triangle) (after [15]).

where S_1 and S_2 are real functions.

According to standard electrodynamics, in the limit of $\omega \to 0$ the real part of the complex conductivity tends to $\sigma_{\rm dc}$, while the imaginary part becomes $-\omega C$, with C the capacitance of the whole system:

$$\sigma(\omega) \to \begin{cases} \sigma_{\rm dc} - i\omega C, & \text{if } p > p_c, \\ -i\omega C, & \text{if } p < p_c \end{cases} \qquad (\omega \to 0). \tag{25}$$

For satisfying these conditions, we must require that $S_1(\tau\omega) \sim (\tau\omega)^{-u}$ above p_c and $S_2(\tau\omega) \sim (\tau\omega)^{1-u}$ below and above p_c. The first condition determines, together with eqs. (15) and (22), the scaling exponent Φ, $\Phi = 1/(\mu + s)$. The second condition yields the new relation for the capacitance [1, 9, 10],

$$C \sim S_2(\tau\omega) \sim |p - p_c|^{(u-1)/\Phi} = |p - p_c|^{-s}, \tag{26}$$

with the same exponent s below and above p_c (see fig. 6). The divergency of C at p_c has a simple physical interpretation: each pair of neighboured clusters forms a capacitor. The effective surface increases when p_c is approached and tends to infinity at p_c. Accordingly, the effective capacitance C of the system also diverges. Next, we discuss a (non-trivial) application of the percolation concept, the ionic transport in dispersed ionic conductors.

1.9 Application of the percolation concept: dispersed ionic conductors

Mixtures of solid ionic conductors (e.g. β-AgI or LiI) with fine particles of an insulating second phase (e.g. Al_2O_3 or SiO_2) can show a marked increase in conductivity as compared to the pure homogeneous system. The ionic conductivity first increases strongly

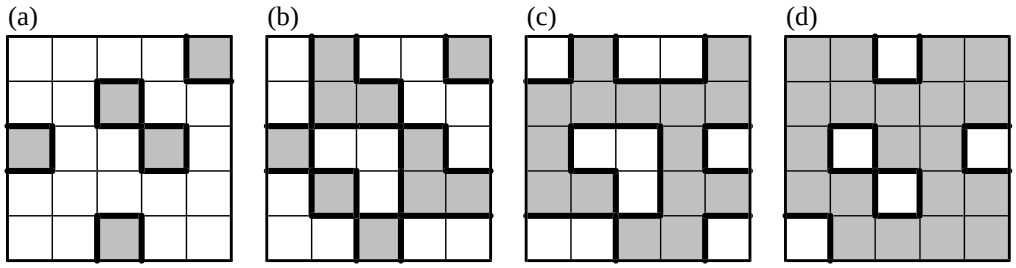

Figure 8 Illustration of the two-phase percolation model on a square lattice for different concentrations p of the insulating material represented by the grey regions. The highly conducting bonds are marked by bold lines. (a) $p < p_c'$, (b) $p = p_c'$, (c) $p = p_c''$, and (d) $p > p_c''$ (redrawn after [15]).

with the concentration p of the dispersed insulating phase. After passing its maximum, the conductivity drops rapidly and seems to approach zero at some larger concentration. The effect is more pronounced as the temperature is lowered [11] (see fig. 7a). The discovery of this remarkable phenomenon is due to Liang [12], who observed an enhancement by three orders of magnitude in the Li conductivity of LiI after addition of Al_2O_3 particles.

It has been shown experimentally for sandwich arrangements of the composites that the interface conductivity between the two phases is strongly enhanced. This enhancement is supposed to be due to the formation of a space charge layer along the internal interfaces [13].

This experimental fact leads to the assumption that the composites can be described as three-component system [14–17] consisting of a matrix of bonds that can be either insulating (representing the interior of the insulating particles), normally conducting with conductivity σ_B^0 (representing the normal conducting bonds), or highly conducting with conductivity $\sigma_A^0 \gg \sigma_B^0$ (representing the interface bonds). The bonds are distributed in space according to a random distribution of insulating material in a normally conducting matrix with a highly conducting interface in between. We shall assume that σ_A^0 and σ_B^0 are thermally activated, such that the ratio $\sigma_A^0/\sigma_B^0 \propto \exp(\Delta E/k_B T)$ increases with decreasing temperature.

Figure 8 shows an illustration of the model on an hypothetical square lattice, for four different concentrations p of the insulating material. For very small p values (fig. 8a) few highly conducting bonds occur and the total conductivity is still dominated by the normal conducting bonds. At some larger p value (fig. 8b) there exists a critical concentration p_c' where for the first time an "infinite" network of highly conducting interface bonds develops ("interface percolation"). For increasing p, the total conductivity increases drastically, since it is now governed by the highly conducting bonds. If we increase p further, we arrive at a second critical concentration p_c'' where all conduction paths become disrupted (fig. 8c). Above p_c'' (fig. 8d), the total conductivity is zero.

Figure 7b shows the results of computer simulations [15] of the total conductivity, carried out on a simple cubic matrix of bonds, for three different temperatures (σ_A^0/σ_B^0=10, 30, and 100). The result compares well with the experimental curve.

Apart from this, the two-phase model is able to reproduce the experimental results for the activation energy as a function of p [18] and the dependence of the specific

conductivity on the size of the dispersed particles [16]. A modified percolation model [17] suggests a cusp in the static effective capacitances.

1.10 Conclusion

In this chapter we gave a short introduction to the standard model for disordered systems, the percolation model. Percolation clusters at the critical concentration are self similar on all length scales and their structure as well as several substructures can be described by fractal geometry. Because the clusters have loops and dangling ends on all length scales diffusion processes on these structures are slowed down on all length scales and become anomalous. Diffusion is related to electrical conductivity via the Nernst-Einstein relation, and thus the scaling behaviour of the dc conductivity can be deduced from it. Other scaling arguments give the dependence of the capacitance on the concentration of conducting sites, and show that the capacitance diverges at the percolation threshold. In the last section, we discussed an application of the percolation concept, ionic transport in dispersed ionic conductors.

1.11 Notation

p, q	concentration of occupied sites, resp. bonds	eqs. 1, 2, 15, 20, 26
P_∞	concentration of sites from the infinite cluster	eq. 1
ξ	correlation length	eq. 2
M	cluster mass	eqs. 3, 4
r, ℓ	Euclidian and topological (chemical) distance	
$R(t) \equiv$		
$\langle r^2(t)\rangle^{1/2}$	root mean square displacement of random walk	eqs. 8, 9, 10
$P(r,t)$	probability density of random walk	eq. 13
D	diffusion coefficient	eqs. 10, 11, 16
$\sigma_{\rm dc}$	dc conductivity	eqs. 11, 15
$\sigma_{\rm S}$	conductivity in conductor-superconductor system	eq. 20
C	capacitance	eq. 26

References

[1] A. Bunde and S. Havlin (eds.), *Fractals and Disordered Systems*, 2nd ed., Springer Verlag, Heidelberg, 1996

[2] D. Stauffer and A. Aharony, *Introduction to Percolation Theory*, Taylor & Francis, London, 1992

[3] M. Sahimi: *Application of Percolation Theory*, Taylor & Francis, London, 1994

[4] S. Alexander and R.L. Orbach, J. Phys. Lett. (Paris) **43** (1982) L625

[5] S. Feng, B.I. Halperin, and P. Sen, Phys. Rev. B **35** (1987) 197

[6] A. Bunde and J. Dräger, Phys. Rev. E **52** (1995) 53

[7] A.M. Dykne, Zh. Eksper. Theor. Fiz. **59** (1970) 111

[8] J.P. Straley, J. Phys. C **9** (1976) 783; Phys. Rev. B **15** (1977) 5733

[9] A.L. Efros and B.I. Shklovskii, Phys. Stat. Sol. B **76** (1976) 475

[10] D. Stroud and D.J. Bergman, Phys. Rev. B **25** (1982) 2061

[11] F.W. Poulsen, N.H. Andersen, B. Kinde, and J. Schoonman, Solid State Ionics **9/10** (1983) 119

[12] C.C. Liang, J. Electrochem. Soc. **120** (1973) 1289

[13] J. Maier, in: *Superionic Solids and Electrolytes*, ed. by A.L. Laskar and S. Chandra, Academic Press, New York, 1989, p. 137

[14] A. Bunde, W. Dieterich and H.E. Roman, Phys. Rev. Lett. **55** (1985) 5; Solid State Ionics **18/19** (1986) 147

[15] H.E. Roman, A. Bunde and W. Dieterich, Phys. Rev. B **34** (1986) 3439

[16] H.E. Roman and M. Yussouf, Phys. Rev. B **36** (1987) 7285

[17] R. Blender and W. Dieterich, J. Phys. C **20** (1987) 6113

[18] Chen Li-Quang et al., Acta Phys. Sin. **34** (1984) 1027